Influence of changes in wetland inundation extent on net fluxes of carbon dioxide and methane in northern high latitudes from 1993 to 2004

2015 Environ. Res. Lett. 10 095009

(http://iopscience.iop.org/1748-9326/10/9/095009)

Environmental Research Letters

LETTER

Influence of changes in wetland inundation extent on net fluxes of carbon dioxide and methane in northern high latitudes from 1993 to 2004

Qianlai Zhuang[1], **Xudong Zhu**[1], **Yujie He**[1], **Catherine Prigent**[2], **Jerry M Melillo**[3], **A David McGuire**[4], **Ronald G Prinn**[5] **and David W Kicklighter**[3]

[1] Purdue Climate Change Research Center and Departments of Earth, Atmospheric and Planetary Sciences and Agronomy, Purdue University, West Lafayette, IN 47907, USA
[2] Laboratoire d'Etudes du Rayonnement et de la Matière en Astrophysique, CNRS, Observatoire de Paris, Paris, France
[3] Ecosystems Center, Marine Biological Laboratory, Woods Hole, MA 02543, USA
[4] US Geological Survey, Alaska Cooperative Fish and Wildlife Research Unit, University of Alaska Fairbanks, Fairbanks, AK 99775, USA
[5] Joint Program on the Science and Policy of Global Change, Massachusetts Institute of Technology, 77 Massachusetts Ave., Cambridge, MA 02139, USA

E-mail: qzhuang@purdue.edu

OPEN ACCESS

RECEIVED
4 May 2015

REVISED
10 August 2015

ACCEPTED FOR PUBLICATION
24 August 2015

PUBLISHED
10 September 2015

Keywords: methane emissions, northern high latitudes, wetland inundation extent, carbon dynamics

Supplementary material for this article is available online

Abstract

Estimates of the seasonal and interannual exchanges of carbon dioxide (CO_2) and methane (CH_4) between land ecosystems north of 45°N and the atmosphere are poorly constrained, in part, because of uncertainty in the temporal variability of water-inundated land area. Here we apply a process-based biogeochemistry model to evaluate how interannual changes in wetland inundation extent might have influenced the overall carbon dynamics of the region during the time period 1993–2004. We find that consideration by our model of these interannual variations between 1993 and 2004, on average, results in regional estimates of net methane sources of 67.8 $\pm$ 6.2 Tg CH_4 yr^{-1}, which is intermediate to model estimates that use two static inundation extent datasets (51.3 $\pm$ 2.6 and 73.0 $\pm$ 3.6 Tg CH_4 yr^{-1}). In contrast, consideration of interannual changes of wetland inundation extent result in regional estimates of the net CO_2 sink of -1.28 ± 0.03 Pg C yr^{-1} with a persistent wetland carbon sink from -0.38 to -0.41 Pg C yr^{-1} and a upland sink from -0.82 to -0.98 Pg C yr^{-1}. Taken together, despite the large methane emissions from wetlands, the region is a consistent greenhouse gas sink per global warming potential (GWP) calculations irrespective of the type of wetland datasets being used. However, the use of satellite-detected wetland inundation extent estimates a smaller regional GWP sink than that estimated using static wetland datasets. Our sensitivity analysis indicates that if wetland inundation extent increases or decreases by 10% in each wetland grid cell, the regional source of methane increases 13% or decreases 12%, respectively. In contrast, the regional CO_2 sink responds with only 7–9% changes to the changes in wetland inundation extent. Seasonally, the inundated area changes result in higher summer CH_4 emissions, but lower summer CO_2 sinks, leading to lower summer negative greenhouse gas forcing. Our analysis further indicates that wetlands play a disproportionally important role in affecting regional greenhouse gas budgets given that they only occupy approximately 10% of the total land area in the region.

1. Introduction

Northern high latitudes (north of 45°N) account for about half of the world's wetlands although their distribution and total area are uncertain (e.g., Bridgham *et al* 2000, Lehner and Döll 2004). These wetlands contain a large amount of soil carbon (Gorham 1991, Vitt *et al* 2000, Turunen *et al* 2002, Warner and Asada, 2006, Tarnocai *et al* 2009) due to low rates of decomposition under anoxic conditions

(Moore *et al* 1998). Traditionally, northern wetlands have been recognized as persistent long-term sinks of carbon (e.g., Smith *et al* 2004). However, they may switch from current sinks to future sources due to changes in soil temperature, moisture, and disturbance regimes (McGuire *et al* 2009, 2012).

To date, the uncertainty of contemporary carbon budgets of northern wetlands is still one of the largest remaining gaps in assessing boreal carbon budgets (e.g., Apps *et al* 1993, Bond-Lamberty *et al* 2006, McGuire *et al* 2009, Fisher *et al* 2014). One of the challenges is to quantify the responses of CO_2 and CH_4 dynamics in highly heterogeneous landscapes to changes in soil thermal and hydrologic regimes caused by changes of climate and land cover in the region. Simultaneous quantification of fluxes of these gases in wetland ecosystems generally has been slow to be incorporated into biogeochemical modeling efforts (Yu 2006). Studies of regional carbon dynamics have primarily focused on quantifying either CO_2 exchanges in uplands (e.g., Clein *et al* 2000, 2002, Lafleur *et al* 2001, Zhuang *et al* 2003, Carrasco *et al* 2006, Balshi *et al* 2007) or CH_4 emissions from wetlands (e.g., Segers and Laffelaar 2001, Walter *et al* 2001, Grant *et al* 2002, Zhuang *et al* 2004, Petrescu *et al* 2010, Melton *et al* 2012). Only a few process-based models have been developed to simulate both CO_2 and CH_4 exchanges, but most of those models have only been applied to a limited number of peatland sites (e.g., Potter *et al* 2001, Zhang *et al* 2002, Fan *et al* 2012). Although a few studies have focused on quantifying the radiative forcing of both CO_2 and CH_4 exchanges in northern ecosystems (e.g., Frolking *et al* 2006, Zhuang *et al* 2006, 2007, Frolking and Roulet 2007), they have not considered how changes in wetland inundation extent affect the simultaneous exchange of CO_2 and CH_4 between land and the atmosphere. With the emerging data on seasonal and inter-annual variation in wetland inundation extent (Prigent *et al* 2001, 2007, Papa *et al* 2010), it is now feasible to evaluate how this variation influences greenhouse gas exchanges in the region.

Here, we conduct such a study with a process-based biogeochemistry model, the Terrestrial Ecosystem Model (TEM, Zhuang *et al* 2004, 2006). Our study focuses on analyzing how inter-annual variations in wetland inundation extent from 1993 to 2004 influence net land fluxes of CO_2 and CH_4 to the atmosphere. Specifically, we compare model simulations driven with three wetland distribution datasets including two synthetic, static wetland distribution products that were developed using various approaches including ground survey and satellite information (Matthews and Fung 1987, Lehner and Döll 2004) and a satellite-based dynamic inundation product with a monthly time step (Prigent *et al* 2007). The comparisons evaluate the impacts of wetland and upland area changes on the net ecosystem carbon exchange, net methane emissions, and their global warming potentials (GWPs) in northern high latitudes.

2. Method

2.1. Overview

Below we briefly describe our methods consisting of: (1) a description of TEM and its modifications to better represent carbon dynamics in wetland ecosystems; (2) our representation of the variations in wetland extent in this study and how it differs from earlier efforts; (3) our representation of the spatial and temporal variation of other environmental factors that influence carbon dynamics in the northern high latitudes; (4) our calculations of regional CO_2 and CH_4 fluxes from the region; and (5) our evaluation of the importance of considering changes in wetland extent on these fluxes. More detailed descriptions of the methods can be found in the supplementary material.

2.2. Model description

The TEM uses spatially-referenced information on climate, elevation, soils, and vegetation to make monthly estimates of vegetation and soil C and nitrogen (N) fluxes and pool sizes. The model is well documented and has been used to examine high latitude terrestrial CO_2 and CH_4 dynamics (e.g., Zhuang *et al* 2003, 2004, 2006, 2007, Euskirchen *et al* 2006, Balshi *et al* 2007, Sitch *et al* 2007, McGuire *et al* 2010). The model explicitly couples biogeochemical processes with soil thermal dynamics of permafrost and non-permafrost soils (figure S1(a)), and is able to simulate the soil temperature profile and the seasonal freeze-thaw depth to define the active layer (Zhuang *et al* 2001, 2002, 2003). The freeze-thaw depth determines the lower boundary of microbial activity in the soil. The density of soil carbon decays exponentially through the soil profile. The biogeochemistry has also been coupled with a sophisticated Hydrological Module (HM, figure S1(a)), which is able to simulate the soil moisture profile and water table depth for both upland and wetland ecosystems. TEM also couples carbon/nitrogen dynamics to the production of methane (figure S1(a)). The Methane Dynamics Module explicitly simulates the processes of CH_4 production (methanogenesis) and CH_4 oxidation (methanotrophy), as well as the transport of the gas between the soil and the atmosphere (figure S1(b), Zhuang *et al* 2004). Various versions of TEM have been applied for quantifying carbon dynamics in boreal regions (e.g., He *et al* 2014, Zhu *et al* 2014). However, these previous model simulations have not explicitly treated the carbon stoichiometry associated with both aerobic and anaerobic decomposition occurring in dynamically changing extent of upland and wetland areas of boreal ecosystems.

In this study, we define net ecosystem exchange (NEE) as the net exchange of CO_2 with the

atmosphere, which is consistent with the definition of NEE by Chapin *et al* (2006). For upland ecosystems, NEE is calculated as the difference between heterotrophic respiration (R_H) and net primary production (NPP). For wetland ecosystems, we extend this definition of NEE to also consider CO_2 emissions due to wetland methane oxidation (R_{CWM}), and CO_2 release accompanied with the production of CH_4 under anaerobic condition (R_{CM}):

$$NEE = R_H + R_{CWM} + R_{CM} - NPP. \quad (1)$$

A negative NEE represents a land sink of atmospheric CO_2 whereas a positive value represents a land source.

2.3. Representation of Wetland inundation extent

To make spatially and temporally explicit estimates of net CO_2 and CH_4 exchanges between the land surface and the atmosphere due to changes in wetland inundation extent in northern high latitudes (north of 45°N), we apply TEM to two datasets of static wetland inundation extent and one time-series dataset where the maximum wetland inundation extent changes annually from 1993 to 2004. The first static wetland inundation extent dataset is extracted from the NASA/GISS global natural wetland dataset at a spatial resolution of 1° × 1° (Matthews and Fung 1987). This dataset is resampled to a spatial resolution of 0.5° × 0.5° (referred to as Wet1). The second static wetland inundation extent dataset is from the Global Lakes and Wetlands Database (GLWD, Lehner and Döll 2004) where we resample a 30 s raster wetland distribution map to a spatial resolution of 0.5° × 0.5° (referred to as Wet2). The time-series dataset of dynamic inundation extent (Papa *et al* 2010) contains the monthly distribution of surface water extent at a ~25 km sampling resolution and we resampled to 0.5° × 0.5° raster maps, which are geographically consistent with Wet1 and Wet2. To associate the inundation data with our model parameterizations for wetland ecosystems, we overlay the monthly changes of inundation extent from 1993 to 2004 to the Wet1 dataset to create 144 monthly maps. The new wetland inundation extent data set (hereafter referred to as Wet3) contains the wetland types defined in Matthews and Fung (1987), but with annual maximum inundation extents (figure S2). Permanent inland water bodies are excluded in the original satellite data (Prigent *et al* 2007). Specifically, for any particular year within the period 1993–2004, an annual map of maximum inundation extent is developed. The annual map consists of the maximum inundation extent for every pixel, which is determined based on its monthly inundation data. These annual maximum inundation extent maps with a mean annual inundation area of 3.15 Mkm^2 are used in Wet3 simulations (figure 1(b)). Note that inundation area for some months could be larger than the static wetland area in Wet1 for some pixels. The extra inundated-area for a particular pixel in the Wet3 data is assumed to be covered with the same wetland types as in the Wet1 data for that pixel.

2.4. Other input datasets

To drive TEM, we also use spatially-explicit data of monthly climate, land cover, soil texture, soil-water pH, elevation, and leaf area index (LAI). The static data sets include potential natural vegetation (Melillo *et al* 1993), soil texture (Zhuang *et al* 2003), and soil-water pH (Carter and Scholes 2000). The historical monthly air temperature, precipitation, vapor pressure, and cloudiness data sets are from the National Centers for Environmental Prediction (http://www.ncep.noaa.gov/). LAI is internally estimated as a function of vegetation carbon within TEM for each 0.5° latitude × 0.5° longitude grid cell. More details about the input data can be found in supplementary material.

2.5. Model parameterization and regional simulations

To conduct the study for the region, which is spatially heterogeneous with respect to land ecosystem types, soils, and climate, we apply the parameterizations for both tundra and boreal forest ecosystems described in previous studies (Zhuang *et al* 2003, 2004) to simulate CH_4 consumption as well as net CO_2 exchanges in upland ecosystems for the corresponding classes in each wetland map. To simulate methane emissions from wetland ecosystems, we use the parameterization of methane dynamics from Zhuang *et al* (2004), in which the simulation of CH_4 emissions was optimized to field measurements at several sites (table S1). To simulate net CO_2 exchanges in wetland ecosystems, we calibrate the revised TEM for three wetland ecosystem types (table S1) including wet tundra wetlands, alpine tundra wetlands, and forested wetlands using a Bayesian inference technique (Tang and Zhuang 2009). Field-based estimates of NEE (table S1) are used to compare with model simulations to optimize TEM parameters.

To examine the effect of inter-annual changes in wetland inundation extent on carbon fluxes, we conduct a 'core' regional simulation with the organized wetland (Wet3) and upland data for the period of 1993–2004. In this simulation, the annual maximum inundation area detected with satellite is treated as wetlands, i.e., the wetland distribution and area change from year to year. To illustrate the effect of the interannual changes of wetland inundation extent, we conduct two other simulations with the 'static' inundation extent datasets Wet1 and Wet2. Each simulation was spun-up for 100 years. For each simulation, the model is run twice for each pixel, once for the upland parameterization and once for the wetland parameterization. In the cases where a grid cell goes

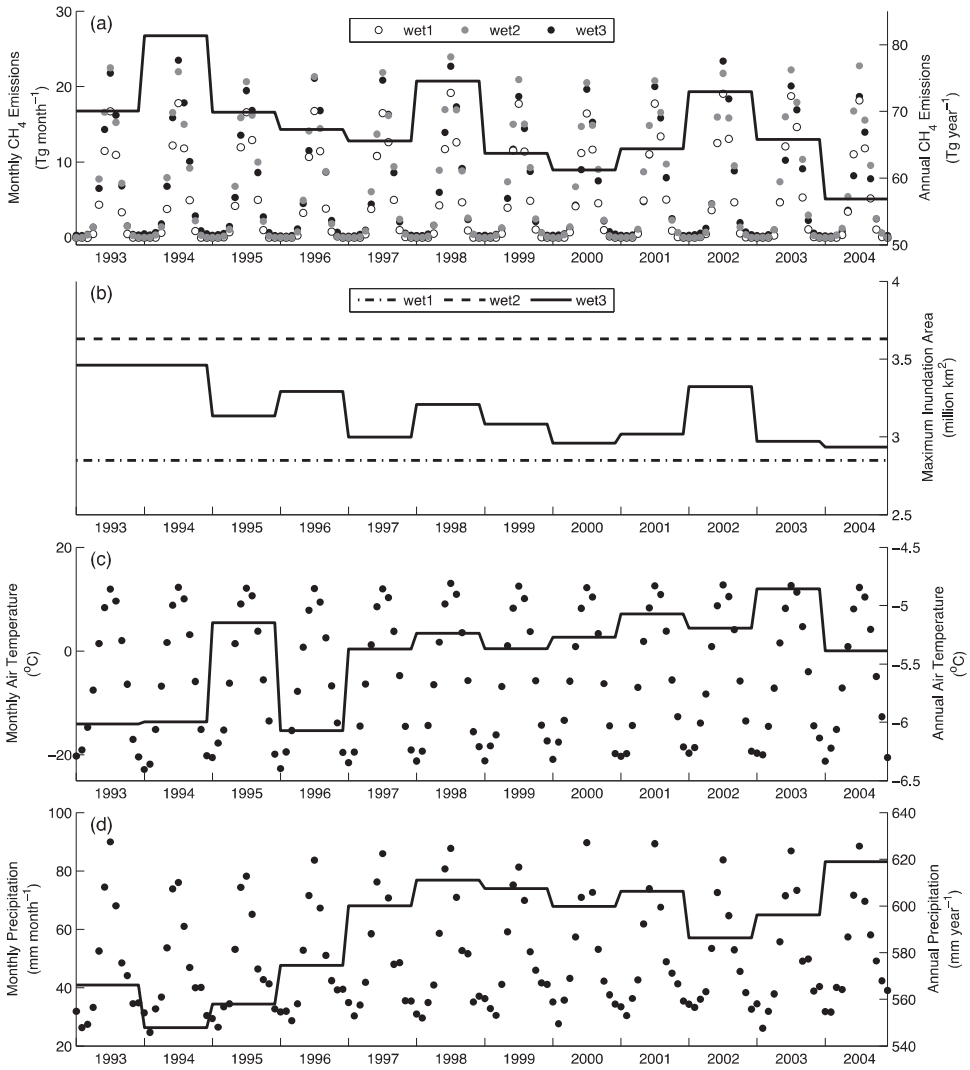

Figure 1. Dynamics of monthly and annual net CH_4 emissions (a), annual maximum wetland inundation areas (b), air temperature (c), and precipitation (d) in the region from 1993 to 2004. Wet1 and Wet2 represent the monthly CH_4 emissions and constant wetland areas for two static wetland datasets. Wet3 represents the monthly CH_4 emissions or maximum dynamic inundation area.

from wetland to upland or from upland to wetland, we multiply the fluxes for each land cover type by the new fraction of wetland and upland.

With the 'core' simulation, we first examine the carbon balance in the region with an explicit consideration of both wetland and upland ecosystems. We then analyze how CO_2 and CH_4 fluxes are related to changes of climate and wetland area extent at an annual time step. In addition, we examine the effects of soil moisture, soil temperature, water table depth, and active layer depth on CO_2 and CH_4 dynamics in the region.

To quantify the sensitivity of both CO_2 and CH_4 fluxes to the uncertain wetland inundation extent in the region, we conduct two additional simulations with slight modifications of the Wet3 dataset. One simulation assumes a 10% increase of the wetland inundation extent for those pixels having wetland distribution in Wet3 whereas the other assumes a 10% decrease in wetland inundation extent. We chose 10% because this value was the approximate percentage change of inundation area between 1993 and 2004.

3. Results

3.1. Inter-annual variation of regional CO_2 and CH_4 dynamics

Driven with the dynamic wetland inundation data, our simulation indicates that inter-annual variations of CH_4 emissions from the land ecosystems in the region range from 56.9 Tg CH_4 yr^{-1} in 2004 to 81.3 Tg CH_4 yr^{-1} in 1994 (table 1). The region acts as a sink of -1.28 ± 0.03 Pg C yr^{-1} for the period of 1993–2004. Wetland ecosystems are persistently a net sink for CO_2 that ranges from -0.38 to -0.41 Pg C yr^{-1} during the period of 1993–2004 for the total area ranging from 2.93 to 3.46 million km^2. The upland ecosystems are also a sink from -0.6 to -1.1 Pg C yr^{-1} for the total area ranging from 37.18 to 37.71 million km^2 over the region (figure 2). The

Table 1. Comparisons of net methane emissions (NME, Tg CH_4 $year^{-1}$) and NEE (Pg C $year^{-1}$) simulated with different wetland scenarios during the period of 1993–2004 in the Pan-Arctic region.

	Static inundation (wet1)			Static inundation (wet2)			Dynamic inundation (wet3)			10% increase of inundation			10% decrease of inundation		
	NME	NEE	GWP	NME	NEE	GWP	NME	NEE	GWP	NME	NEE	GWP	NME	NEE	GWP
1993	47.4	−1.24	−3.36	72.5	−1.34	−3.10	70.0	−1.27	−2.91	78.8	−1.38	−3.07	61.3	−1.18	−2.80
1994	51.7	−1.23	−3.22	74.7	−1.34	−3.05	81.3	−1.26	−2.59	91.5	−1.36	−2.72	71.2	−1.17	−2.51
1995	52.0	−1.31	−3.50	73.0	−1.43	−3.42	69.9	−1.31	−3.06	78.7	−1.42	−3.23	61.2	−1.22	−2.93
1996	46.8	−1.23	−3.34	66.0	−1.34	−3.26	67.3	−1.23	−2.83	75.8	−1.33	−2.99	58.9	−1.14	−2.72
1997	49.7	−1.26	−3.38	70.8	−1.38	−3.29	65.6	−1.24	−2.91	73.8	−1.34	−3.08	57.4	−1.15	−2.79
1998	53.5	−1.31	−3.47	80.1	−1.42	−3.20	74.5	−1.30	−2.90	83.9	−1.41	−3.07	65.2	−1.21	−2.80
1999	50.6	−1.30	−3.50	72.2	−1.42	−3.40	63.7	−1.29	−3.14	71.7	−1.40	−3.33	55.8	−1.20	−3.00
2000	49.5	−1.28	−3.46	70.0	−1.40	−3.38	61.2	−1.24	−3.02	68.9	−1.34	−3.20	53.6	−1.15	−2.89
2001	53.2	−1.28	−3.36	74.6	−1.40	−3.27	64.4	−1.27	−3.05	72.5	−1.38	−3.23	56.4	−1.18	−2.92
2002	53.7	−1.27	−3.31	69.7	−1.39	−3.35	73.0	−1.28	−2.87	82.2	−1.39	−3.03	63.9	−1.19	−2.76
2003	56.5	−1.39	−3.68	78.0	−1.50	−3.55	65.8	−1.36	−3.34	74.1	−1.47	−3.55	57.6	−1.26	−3.19
2004	50.7	−1.32	−3.57	74.4	−1.44	−3.42	56.9	−1.29	−3.31	64.1	−1.40	−3.52	49.8	−1.20	−3.15
Mean	51.3	−1.29	−3.43	73.0	−1.40	−3.31	67.8	−1.28	−2.99	76.3	−1.39	−3.17	59.4	−1.19	−2.87
Std	2.60	0.04	0.12	3.60	0.05	0.14	6.20	0.03	0.20	7.00	0.04	0.22	5.40	0.03	0.18

Note: Global warming potential (GWP, Pg CO_2 equivalents $year^{-1}$) is calculated on a 100-year time horizon, i.e., 1 g of CH_4 is equivalent to 25 g of CO_2 (IPCC 2007). Negative NEE/GWP indicates a sink of greenhouse gases from the atmosphere and positive NEE/GWP indicates a source of greenhouse gases to the atmosphere.

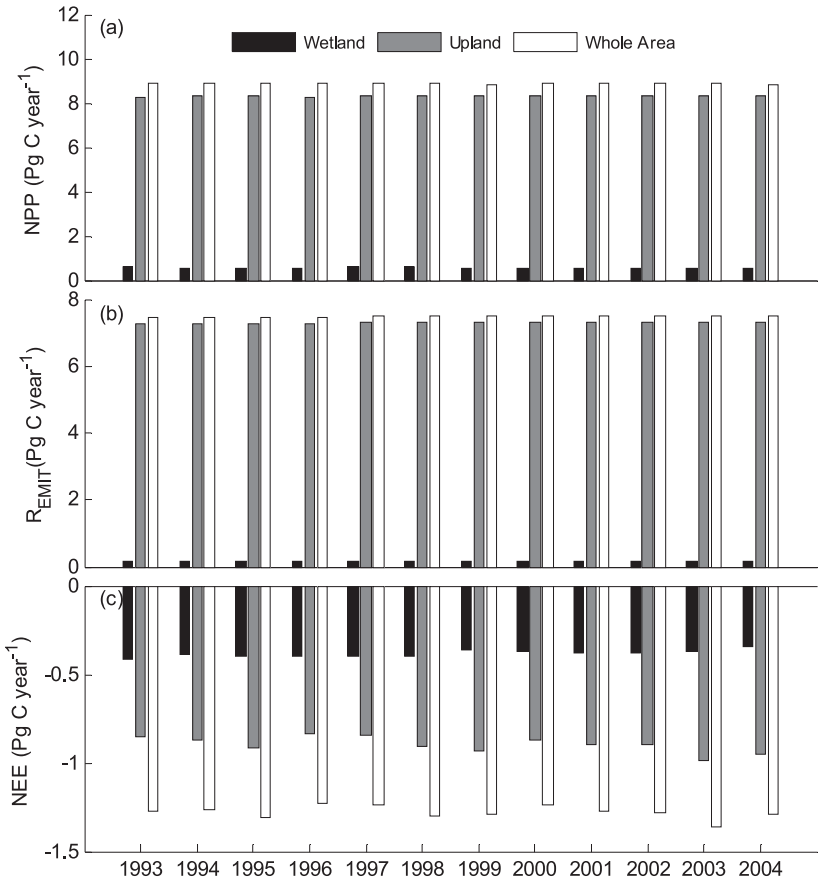

Figure 2. Annual carbon fluxes due to changes of climate and wetland inundation extent (Wet3) from 1993 to 2004 in wetland, upland, and the whole region for (a) NPP (CO_2–C), (b) R_{EMIT} (CO_2–C), and (c) NEE (CO_2–C). Here, $R_{EMIT} = R_H$ for uplands, while $R_{EMIT} = R_H + R_{CWM} + R_{CM}$ for wetlands, see equation (1).

inter-annual variation in net CH_4 emissions of the entire region is significantly correlated with annual maximum wetland inundation extent and inversely correlated with annual precipitation, but there is no significant correlation with the annual air temperature (table 2). It is not clear why annual precipitation and annual inundation extent are not correlated. It is possible that the variability in annual inundation extent is determined by seasonal patterns in precipitation (e.g., rain in late summer or high snow pack in winter), which may not necessarily correlate with annual precipitation. There are also no significant correlations of annual CH_4 emissions with the mean annual soil temperature at depth 20 cm, active layer depth, and water table depth. Inter-annual variation in NEE is not significantly correlated with these environmental variables except wetlands area at the annual temporal resolution.

The spatial patterns of exchanges of CO_2 and CH_4 (figure S3) vary depending on the wetland inundation extent, which fluctuates in the region (figure S2). Both CO_2 and net CH_4 emissions exhibit a significant spatial variability as demonstrated with two inundation extent extreme years 1994 (the highest) and 2004 (the lowest). During 1994, a larger wetland inundation area estimates a higher methane production and emissions (81.3 Tg CH_4 yr^{-1}). For CO_2 dynamics, the region acts as a carbon sink of -1.26 Tg C yr^{-1} as a balance of a wetland sink of -0.41 Pg C yr^{-1} and an upland sink of -0.85 Pg C yr^{-1} (figure 2). In contrast, the smallest wetland inundation extent in 2004 estimates the regional net methane emissions as small as 56.9 Tg CH_4 yr^{-1} (figure 1, table 1). The NEE is a sink of -1.29 Pg C yr^{-1} as a result of both uplands and wetlands sinks (figure 2).

There are large differences in net methane emissions and net carbon exchanges under static and dynamical wetland inundation conditions (table 1). Under the 'static' wetland inundation extent conditions Wet1 and Wet2, the regional methane emissions range from 51.3 ± 2.6 to 73.0 ± 3.6 Tg CH_4 yr^{-1} during the period of 1993–2004 (figure S4(a)). For NEE, the region acts as a persistent sink ranging from -1.29 ± 0.04 to -1.40 ± 0.05 Pg C yr^{-1} under static wetland inundation conditions (table 1).

3.2. Seasonal dynamics of CO_2 and CH_4 in the region

All three 'core' simulations show a similar seasonal CH_4 emission pattern, peaking in July (figure S4(b)). In wetland areas, the carbon sink corresponds to the size of wetlands in three simulations in summer months (figure S5(a)). The sink estimates range from

Table 2. Pearson correlations (R) of simulated annual ($n = 12$) net methane emissions, NEE, and GWP with environmental variables based on satellite-detected annual maximum inundation extent data for the study region from 1993 to 2004.

	Wetland areas	Precipitation	Air temperature	Soil temperature at depth 20 cm	Soil moisture at depth 20 cm	Active layer depth	Water table depth
Net CH_4 emissions	0.81[b]	−0.68[a]	−0.34	−0.31	−0.45	0.01	−0.10
NEE	0.13[a]	−0.07	−0.57	−0.56	0.12	−0.35	−0.21
GWP	0.78[b]	−0.62[a]	−0.65	−0.62[a]	−0.31	−0.22	−0.22

[a] P-value less than 0.05.

[b] P-value less than 0.01.

−0.1 to −0.2 Pg C month^{-1} in June and July. Wetland NEE is similar between the three simulations from January through May, and September through December (figure S5(a)). In contrast, changes in the extent of uplands do not result in substantial differences in NEE between the three simulations (figure S5 (b)). As a result, changes of annual inundation extent result in seasonal NEE differences up to 0.04 Pg C month^{-1} in the region (figure S5(c)). Overall, the inundated area changes result in higher summer CH_4 emissions, but lower summer NEE sinks (figures S4 and S5).

3.3. Sensitivity of net exchanges of CO_2 and CH_4

For a 10% change in annual maximum wetland inundation extent, our simulations indicate that the regional net exchanges of CO_2 and CH_4 are affected by subsequent changes of wetland and upland areas (table 1). Net exchanges of CH_4 are more sensitive to wetland inundation extent changes than NEE. Specifically, if wetland inundation extent increases or decreases by 10% in each wetland grid cell, the regional source of methane increases 13% or decreases 12%, respectively. In contrast, the regional NEE responds with only 7–9% changes to the changes in wetland inundation extent (table 1). The response of net CH_4 emissions is mainly due to the stronger effect of the changes in inundated areas on methane production than on methane consumption as methane consumption in uplands is an order of magnitude less than wetland methane production (see figure 3). The response of regional NEE to changes in wetland inundation area is dominated by the response of aerobic decomposition to changing wetland area. Upland area changes due to changing inundation area are relatively small given that the upland area is much larger than wetland area, the upland NEE thus does not change significantly.

4. Discussion and summary

4.1. Regional wetland emissions and atmospheric concentrations of CH_4

Nine inversion studies estimated that net CH_4 emissions of boreal region wetlands are 34 ± 13 Tg CH_4 yr^{-1} (Chen and Prinn 2006). Another inversion constrained by atmospheric observations of methane and its $^{13}C/^{12}C$ isotopic ratio data indicates that the boreal region releases 30–64 Tg CH_4 yr^{-1}, presumably mainly from wetlands (Mikaloff Fletcher *et al* 2004, McGuire *et al* 2012). A more recent study using satellite data estimated that mean summer emissions are 53 Tg CH_4 yr^{-1} from boreal-Arctic wetlands (Watts *et al* 2014). The 'static' wetland inundation dataset Wet1 estimates CH_4 emissions that are comparable with the various inversions, while both Wet2 and dynamic wetland inundation extent dataset Wet3 estimates much higher emissions due to the larger wetland or inundated area in the latter two datasets (table 1). Annual emissions correlate well with annual wetland inundation area. In particular, the highest emissions occur in 1994, which is primarily explained by the largest inundation area in the period. Both static and dynamic wetland simulations estimate higher emissions in 1998 than in 1999, which is consistent with the inversion results (e.g., Mikaloff Fletcher *et al* 2004, Chen and Prinn 2006). While annual maximum wetland inundation area is larger in 1998 than in 1999, so are the annual precipitation and air temperature (figures 1(c) and (d)), suggesting that climatic conditions in 1998 also favor the methane emissions. A number of studies have suggested that the difference in CH_4 emissions between 1998 and 1999 is the responses to temperature changes associated with the warm conditions in 1998 due to the strong El Niño phenomena (e.g., Dlugokencky *et al* 2001, Cunnold *et al* 2002). Indeed, 1998 was marked with elevated temperatures in the region from June to August (Bell *et al* 1999), and its annual temperature was higher than the 12-year average annual temperature over the region and the annual temperature of 1999. In addition, some high northern latitudes regions experienced elevated precipitation from April to September, which might have also led to the elevated wetland emissions for the year 1998 (Curtis *et al* 2001, Dlugokencky *et al* 2001). Our analysis indicates that precipitation in 1998 is indeed higher than in year 1999 while air temperature and inundated land area is also above the average of the study period (figure 1(d)). The temperature and wetland inundation responses together dominate the positive anomaly of net methane emissions for the year 1998 in the region.

Our simulations further indicate that the three wetland datasets estimate similar seasonal dynamics of methane emissions with different magnitudes over the region (figure S4(b)). The peak emissions occur in July. These seasonal dynamics are dominated by climatic factors, rather than wetland inundation extent. To consider the seasonal rather than annual wetland inundation extent in a future analysis will improve the estimates of seasonal dynamics. To date, most atmospheric transport chemistry and inversion models have primarily based their analyses on methane fluxes estimated without considering changes of wetland inundation extent (e.g., Houweling *et al* 1999, Cunnold *et al* 2002, Dentener *et al* 2003, Wang *et al* 2004, Chen and Prinn 2005, 2006). Coupling estimates of methane emissions considering both seasonal and interannual wetland inundation extent dynamics with these atmospheric models should improve modeling atmospheric methane concentrations.

4.2. Regional NEE

Our estimates of NEE account for the CO_2 emissions from both aerobic decomposition and anaerobic

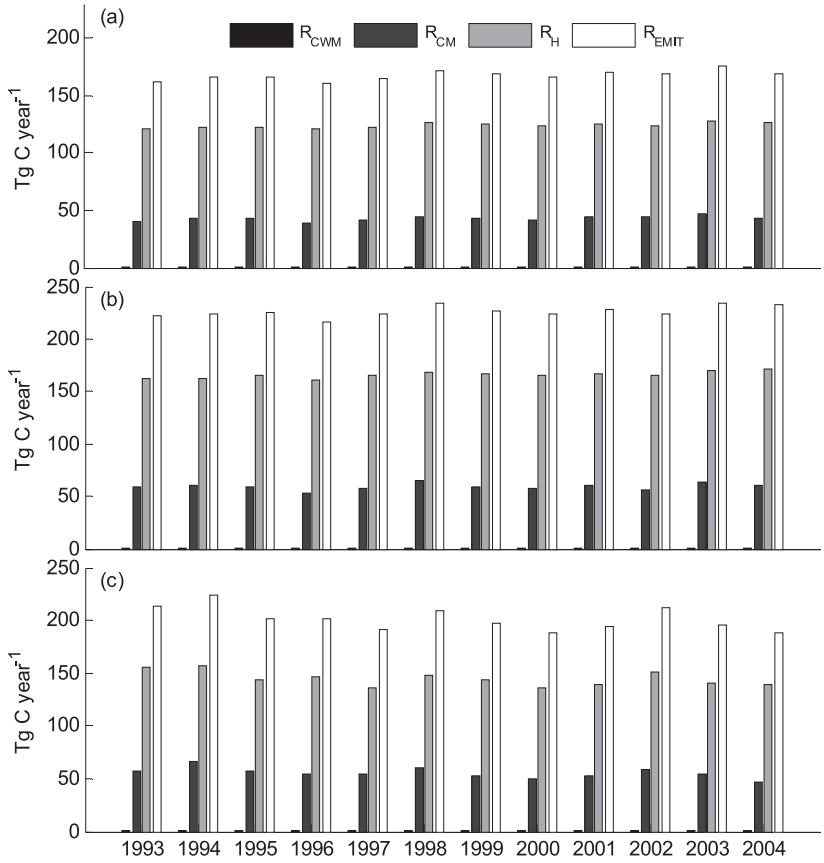

Figure 3. Inter-annual variations of wetland emissions of carbon dioxide (R_{EMIT}) partitioned to aerobic emissions (R_H) from the unsaturated zone of the wetland soil profile due to fluctuations of water table depth, the emissions accompanied with methane oxidation (R_{CWM}), and the emissions accompanied with the methane production (R_{CM}) from 1993 to 2004 for (a) Wet1, (b) Wet2, and (c) Wet3.

decomposition of the soils (see equation (1)). Based on the static wetland inundation extent of the Wet1 and Wet2 datasets, the region is estimated to be a consistent sink (table 1). The annual NEE ranges from -1.23 to -1.50 Pg C yr^{-1} for the period 1993–2004. The dynamic wetland inundation extent estimates the region to be a similar sink at -1.28 ± 0.03 Pg C yr^{-1}. The larger regional sink under static wetland inundation conditions is due to the larger wetland area prescribed by the Wet2 dataset that enhances the carbon sink. The smaller regional sink is mainly due to the decrease of the regional wetland carbon sink as wetlands area decreases under the dynamic wetland inundation condition. Although the wetland area is much smaller than the upland area in this region and both NPP and R_H of upland are much higher than that of wetlands, the strength of the carbon sink of the wetlands account for about one-third of the total regional sink. For instance, the sink of wetlands (-0.42 Pg C yr^{-1} or 126.4 g C m^{-2} yr^{-1}) of 2002 is about half of the upland sink (figure 2(c)). This suggests that the wetland ecosystems play a disproportional role in affecting regional NEEs. Breakdown of the wetland emissions of CO_2 shows that the majority of emissions are from the unsaturated zone of the wetland soils, which is created with the fluctuation of water table depth (figure 3). This aerobic decomposition accounts for 80% of the total wetland CO_2 emissions while the release of carbon associated with the methane oxidation and production varies between 40 and 60 Tg C yr^{-1} with wetland inundation extents.

In comparison with an earlier estimate of a sink of 51.1 Tg C yr^{-1} over the 1997–2006 time period (McGuire *et al* 2010), our estimated regional NEE magnitudes based on the satellite-detected dynamic wetland extent dataset are much larger. If we account for fire emissions (246.5 Tg C yr^{-1}) and the decomposition of agricultural and forestry products (13.5 Tg C yr^{-1}) estimated by McGuire *et al* (2010) for the same region in our analysis, our estimates of NEE will be a large sink of -1.0 Pg C yr^{-1} under the dynamic wetland conditions. A recent inter-model comparison shows that the multi-model mean annual NEE for Alaska is largely carbon neutral (Fisher *et al* 2014) while some observations suggest that portions of the region have been a source of CO_2 to the atmosphere (Oechel *et al* 2000, 2014). The differences of carbon budget estimates between various models and our estimates are at least due to: (1) different processes being considered by the models; (2) different models parameterizations; (3) different sensitivity of the models to the same forcing data; and (4) different

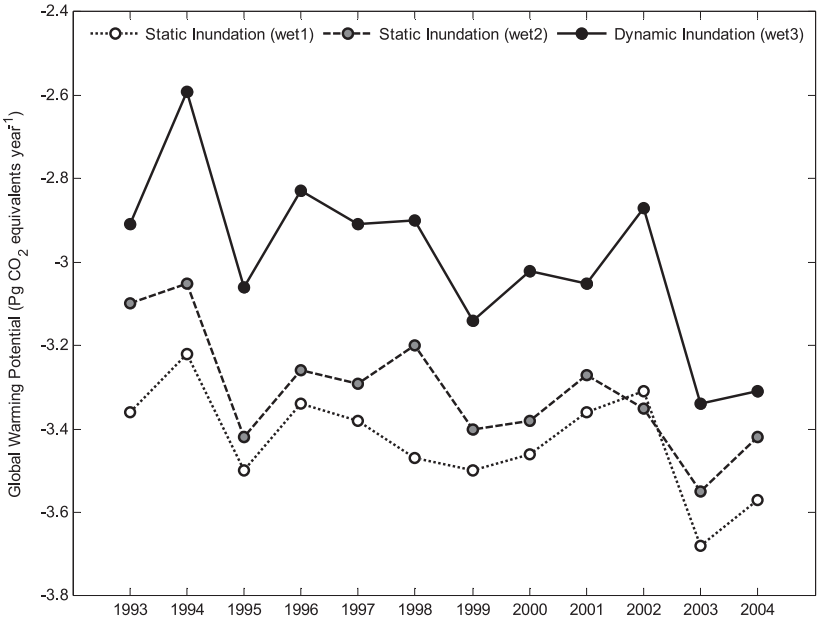

Figure 4. Inter-annual variations of global warming potentials (GWP) of the Pan-Arctic under 'static' and dynamic wetland inundation conditions from 1993 to 2004. Negative values indicate a sink and positive values indicate a source of these gases.

treatment of land ecosystems (e.g., the inundated area changing) among the models (Melton *et al* 2012, Bohn *et al* 2015). The TransCom model means for the period of 1995–2006 for the region range from a source of 0.03 Pg C yr^{-1} to a sink of −0.89 Pg C yr^{-1} with a large uncertainty (Gurney *et al* 2004, 2008). Using the estimates of NEE that consider the effects of wetland inundation extent changes and both aerobic and anaerobic decomposition as priors for atmospheric inversion modeling may reduce the current discrepancy between process-based biogeochemical modeling and inversion estimates.

4.3. Regional GWPs of CO_2 and CH_4

Previous evaluation of regional radiative forcing estimated as GWPs was based on regional methane emissions and NEEs that have not considered changes in wetland inundation extent (e.g., Zhuang *et al* 2007). Consideration of wetland inundation dynamics reduced the estimated regional negative climate forcing (figure 4, table 1). Overall, the estimated regional GWP sink using either static or dynamic inundated area data increases during the study period (figure 4). The increase estimated using dynamic inundation data is mainly due to the decrease of CH_4 emissions resulting from the declining inundated area (figure 1). The slight increase estimated using two static wetland datasets is due to the slight increase of the carbon sink (table 1). Our sensitivity analysis indicates that the regional GWP under the conditions of either a 10% increase or a 10% decrease in inundation area of the Wet3 dataset differs little (less than 6%) from the estimates with Wet3 (table 1). Thus, changes in CH_4 fluxes associated with a 10% change in wetland inundation extent appear to compensate for changes in CO_2 fluxes. This suggests that rather large changes in wetland inundation extent would be required to significantly alter the balance of NEE and methane emissions and to influence the GWP in the region. The heterogeneity of NEE and methane emissions as wetland and upland fractions change inter-annually across the landscape as well as climatic changes results in a large spatial variability in GWP across the pan-Arctic (figure S3).

The regional annual GWP is significantly correlated with interannual wetland inundation extent (table 2). Net methane emissions correlate with wetland inundation extent more significantly than NEE, which suggests that future changes of wetland inundation extent will greatly affect regional net ecosystem carbon and CH_4 exchanges at annual scales. If wetland inundation extent increases, there will be more regional CH_4 emissions, but less regional CO_2 emissions from a relatively smaller upland area and a stronger carbon sink in a relatively larger wetland area. As a result, the regional GWP source will be weaker (figure 4). Future climate predictions with general circulation models therefore should consider the feedback that is induced by these CO_2 and CH_4 dynamics under changing wetland areas in addition to the physical feedbacks of wetland distribution (e.g., Gutowski *et al* 2007, Prigent *et al* 2011).

It is important to note that the greatest limitation of this analysis is the use of relatively coarse resolution (i.e., 0.5° × 0.5°) wetland inundation datasets, which do not capture small features within wetlands that create CH_4 hotspots. An average wetness across these large pixels is also likely to underestimate actual CH_4 fluxes (e.g. Becker *et al* 2008, Baird *et al* 2009).

Additional studies are needed to analyze how these small-scale features of wetlands affect our analysis.

This study considers the influence of water table depth and the stoichiometry of CO_2 and CH_4 during soil anaerobic and aerobic decomposition processes in developing regional estimates of CO_2 and CH_4 fluxes. The study shows that the use of satellite-detected wetland inundation extent essentially reduces the regional GWP sink estimated using static wetland inundation extent data sets and the regional dynamics of CO_2 and CH_4 respond differently to changes of wetland inundation extent with CH_4 fluxes being more sensitive than CO_2 fluxes. Future studies should thus consider the dynamics of wetland inundation extent in quantifying both net CO_2 and CH_4 fluxes and their feedbacks to the atmospheric climate and chemistry at regional and global scales. Inundation area data developed from satellite sensors such as NASA Soil Moisture Active Passive will be valuable for making additional progress on understanding how inundation area influences greenhouse gas exchange in the study region.

Acknowledgments

This research is supported by the NASA Land Use and Land Cover Change program (NASA-NNX09AI26G), Department of Energy (DE-FG02-08ER64599), National Science Foundation (NSF-1028291 and NSF-0919331), the NSF Carbon and Water in the Earth Program (NSF-0630319), and the NSF Division of Information & Intelligent Systems (IIS-1028291). The computing is supported by Rosen Center of high performance computing at Purdue. Any use of trade, firm, or product names is for descriptive purposes only and does not imply endorsement by the US Government.

References

Apps M J, Kurz W A, Luxmoore R J, Nilsson L O, Sedjo R A, Schmidt R, Simpson L G and Vinson T S 1993 Boreal forests and tundra *Water Air Soil Pollut.* **70** 39–53

Baird A J, Belyea L R and Morris P J 2009 Upscaling of peatland-atmosphere fluxes of methane *Small-Scale Heterogeneity in Process Rates and the Pitfalls of 'Bucket-and-Slab' Models, Carbon Cycling in Northern Peatlands* (*Geophysical Monograph Series*) vol 184 ed A J Baird *et al* (Washington, DC: AGU) pp 37–53

Balshi M S *et al* 2007 The role of historical fire disturbance in the carbon dynamics of the pan-boreal region: a process-based analysis *J. Geophys. Res.* **112** G02029

Becker T, Kutzbach L, Forbrich I, Schneider J, Jager D, Thees B and Wilmking M 2008 Do we miss the hot spots?—the use of very high resolution aerial photographs to quantify carbon fluxes in peatlands *Biogeosciences* **5** 1387–93

Bell G D, Halpert M S, Ropelewski C F, Kousky V E, Douglas A V, Schnell R C and Gelman M E 1999 Climate assessment for 1998 *Bull. Am. Meteorol. Soc.* **80** S1–48

Bohn T J *et al* 2015 WETCHIMP-WSL: intercomparison of wetland methane emissions models over West Siberia *Biogeosciences* **12** 3321–49

Bond-Lamberty B, Gower S T, Goulden M K and McMillan A 2006 Simulation of boreal black spruce chronosequences: comparison to field measurements and model evaluation *J. Geophys. Res.* **111** G2014

Bridgham S D, Ping C-L, Richardson J L and Updegraff K 2000 Soils of northern peatlands: Histosols and Gelisols *Wetland Soils: Genesis, Hydrology, Landscapes, and Classification* ed J L Richardson and M J Vepraskas (Boca Raton, FL: CRC Press) pp 343–70

Carrasco J J, Neff J C and Harden J W 2006 Modeling physical and biogeochemical controls over carbon accumulation in a boreal forest soil *J. Geophys. Res.* **111** G02004

Carter A J and Scholes R J 2000 *Soildata V2.0: Generating a Global Database of Soil Properties* (South Africa: CSIR Environmentek)

Chapin F S III *et al* 2006 Reconciling carbon-cycle concepts, terminology, and methods *Ecosystems* **9** 1041–50

Chen Y-H and Prinn R G 2005 Atmospheric modeling of high- and low-frequency methane observations: importance of interannually varying transport *J. Geophys. Res.* **110** D10303

Chen Y-H and Prinn R G 2006 Estimation of atmospheric methane emissions between 1996 and 2001 using a three-dimensional global chemical transport model *J. Geophys. Res.* **111** D10307

Clein J S, McGuire A D, Zhang X, Kicklighter D W, Melillo J M, Wofsy S C, Jarvis P G and Massheder J M 2002 Historical and projected carbon balance of mature black spruce ecosystems across North America: the role of carbon–nitrogen interactions *Plant Soil* **242** 15–32

Clein J S, Kwiatkowski B L, McGuire A D, Hobbie J E, Rastetter E B, Melillo J M and Kicklighter D W 2000 Modeling carbon responses of moist tundra ecosystems to historical and projected climate: a comparison of fine- and coarse-scale ecosystem models for identification of process-based uncertainties *Glob. Change Biol.* **6** 127–40

Cunnold D M *et al* 2002 *In situ* measurements of atmospheric method at GAGE/AGAGE sites during 1985–2000 and resulting source inferences *J. Geophys. Res.* **107** 4225

Curtis S, Adler R, Huffman G, Nelkin E and Bolvin D 2001 Evolution of tropical and extratropical precipitation anomalies during the 1997–1999 ENSO cycle *Int. J. Climatol.* **21** 961–7

Dentener F, van Weele M, Krol M, Houweling S and van Velthoven P 2003 Trends and inter-annual variability of methane emissions derived from 1979–1993 global CTM simulations *Atmos. Chem. Phys.* **3** 73–88

Dlugokencky E J, Walter B P, Masarie K A, Lang P M and Kasischke E S 2001 Measurements of an anomalous global methane increase during 1998 *Geophys. Res. Lett.* **28** 499–502

Euskirchen E S *et al* 2006 Importance of recent shifts in soil thermal dynamics on growing season length, productivity, and carbon sequestration in terrestrial high-latitude ecosystem *Glob. Change Biol.* **12** 731–50

Fan Z, McGuire A D, Turetsky M R, Harden J W, Waddington J M and Kane E S 2012 The response of soil organic carbon of a rich fen peatland in interior Alaska to projected climate change *Glob. Change Biol.* **19** 604–20

Fisher J B *et al* 2014 Carbon cycle uncertainty in the Alaskan Arctic *Biogeosciences* **11** 4271–88

Frolking S, Roulet N and Fuglestvedt J 2006 How northern peatlands influence the Earth's radiative budget: sustained methane emission versus sustained carbon sequestration *J. Geophys. Res.* **111** G01008

Frolking S and Roulet N T 2007 Holocene radiative forcing impact of northern peatland carbon accumulation and methane emissions *Glob. Change Biol.* **13** 1079–88

Gorham E 1991 Northern peatlands: Rolein the carbon cycle and probable responses to climatic warming *Ecol. Appl.* **1** 182–95

Grant R, Roulet N T and Crill P 2002 Methane efflux from boreal wetlands: theory and evaluating the ecosystem model ecosys with chamber and tower flux measurements *Glob. Biogeochem. Cycles* **16** 2001GB001702

Gurney K R *et al* 2004 Transcom 3 inversion intercomparison: modelmean results for the estimation of seasonal carbon sources and sinks *Glob. Biogeochem. Cycles* **18** GB1010

Gurney K R, Baker D, Rayner P and Denning S 2008 Interannual variations in continental-scale net carbon exchange and sensitivity to observing networks estimated from atmospheric CO_2 inversions for the period 1980–2005 *Glob. Biogeochem. Cycles* **22** GB3025

Gutowski W J, Wei H, Vörösmarty C J and Fekete B M 2007 Influence of Arctic Wetlands on Arctic atmospheric circulation. *J. Clim.* **20** 4243–54

He Y, Jones M, Zhuang Q, Bochicchio C, Felzer B S, Mason E and Yu Z 2014 Evaluating CO_2 and CH_4 dynamics of Alaskan ecosystems during the Holocene thermal maximum *Quat. Sci. Rev.* **86** 63–77

Houweling S, Kaminski T, Dentener F, Lelieveld J and Heimann M 1999 Inverse modeling of methane sources and sinks using the adjoint of a global transport model *J. Geophys. Res.* **104** 26137–60

IPCC 2007 *Climate Change 2007: The Physical Science Basis. Contribution of Working Group I to the Fourth Assessment Report of the Intergovernmental Panel on Climate Change* ed Solomon *et al* (Cambridge: Cambridge University Press)

Lafleur P M, Roulet N T and Admiral S W 2001 The annual cycle of CO_2 exchange at a boreal bog peatland *J. Geophys. Res.* **106** 3071–81

Lehner B and Döll P 2004 Development and validation of a global database of lakes, reservoirs and wetlands *J. Hydrol.* **296** 1–22

Matthews E and Fung I 1987 Methane emissions from natural wetlands: global distribution, are, and environmental characteristics of sources *Glob. Biogeochem. Cycles* **1** 61–86

McGuire A D *et al* 2010 An analysis of the carbon balance of the Arctic Basin from 1997–2006 *Tellus* B **62** 455–74

McGuire A D *et al* 2012 An assessment of the carbon balance of Arctic tundra: comparisons among observations, process models, and atmospheric inversions *Biogeosciences* **9** 3185–204

McGuire A D, Anderson L G, Christensen T R, Dallimore S, Guo L, Hayes D J, Heimann M, Lorenson T D, Macdonald R W and Roulet N 2009 Sensitivity of the carbon cycle in the Arctic to climate change *Ecol. Monogr.* **79** 523–55

Melillo J M, McGuire A D, Kicklighter D W, Moore B III, Vorosmarty C J and Schloss A L 1993 Global climate change and terrestrial net primary production *Nature* **363** 234–40

Melton J R *et al* 2012 Present state of global wetland extent and wetland methane modelling: conclusions from a model intercomparison project (WETCHIMP) *Biogeosci. Discuss.* **9** 11577–654

Mikaloff Fletcher S E, Tans P P, Bruhwiler L M, Miller J B and Heimann M 2004 CH_4 sources estimated from atmospheric observations of CH_4 and its $^{13}C/^{12}C$ isotopic ratios: 2. Inverse modeling of CH_4 fluxes from geographic regions *Glob. Biogeochem. Cycles* **18** GB4005

Moore T R, Roulet N T and Waddington J M 1998 Uncertainties in predicting the effect of climatic change on the carbon cycling of Canadian peatlands *Clim. Change* **40** 229–45

Oechel W C, Laskowski C A, Burba G, Gioli B and Kalhori A A 2014 Annual patterns and budget of CO_2 flux in an Arctic tussock tundra ecosystem *J. Geophys. Res.* **119** 323–39

Oechel W C, Vourlitis G L, Hastings S J, Zulueta R C, Hinzman L and Kane D 2000 Acclimation of ecosystem CO_2 exchange in the Alaskan Arctic in response to decadal climate warming *Nature* **406** 978–81

Papa F, Prigent C, Aires F, Jimenez C, Rossow W B and Matthews E 2010 Interannual variability of surface water extent at the global scale 1993–2004 *J. Geophys. Res.* **115** D12111

Petrescu A M R, van Beek L P H, van Huissteden J, Prigent C, Sachs T, Corradi C A R, Parmentier F J W and Dolman A J 2010 Modeling regional to global CH_4 emissions of boreal and arctic wetlands *Glob. Biogeochem. Cycles* **24** GB4009

Potter C, Bubier J L, Crill P M and Lafleur P 2001 Ecosystem modeling of methane and carbon dioxide fluxes for boreal forest sites *Can. J. For. Res.* **31** 208–23

Prigent C, Matthews E, Aires F and Rossow W B 2001 Remote sensing of global wetland dynamics with multiple satellite data sets *Geophys. Res. Lett.* **28** 4631–4

Prigent C, Papa F, Aires F, Rossow W B and Matthews E 2007 Global inundation dynamics inferred from multiple satellite observations, 1993–2000 *J. Geophys. Res.* **112** D12107

Prigent C, Rochetin N, Aires F, Defer E, Grandpeix J-Y, Jimenez C and Papa F 2011 Impact of the inundation occurrence on the deep convection at continental scale from satellite observations and modeling experiments *J. Geophys. Res.* **116** D24118

Segers R and Leffelaar P A 2001 Modeling methane fluxes in wetlands with gas-transporting plants 3. Plot scale *J. Geophys. Res.* **106** 3541–58

Sitch S, McGuire A D, Kimball J, Gedney N, Gamon J, Engstrom R, Wolf A, Zhuang Q, Clein J and McDonald K C 2007 Assessing the carbon balance of circumpolar arctic tundra using remote sensing and process modeling *Ecol. Appl.* **17** 213–34

Smith L C, MacDonald G M, Velichko A A, Beilman D W, Borisova O K, Frey K E, Kremenetski K V and Sheng Y 2004 Siberian peatlands a net carbon sink and global methane source since the early Holocene *Science* **303** 353–6

Tang J and Zhuang Q 2009 A global sensitivity analysis and Bayesian inference framework for improving the parameter estimation and prediction of a process-based Terrestrial ecosystem model *J. Geophys. Res.* **114** D15303

Tarnocai C, Canadell J G, Schuur E A G, Kuhry P, Mazhitova G and Zimov S 2009 Soil organic carbon pools in the northern circumpolar permafrost region *Glob. Biogeochem. Cycles* **23** GB2023

Turunen J, Tomppo E, Tolonen K and Reinikainen A 2002 Estiamting carbon accumualtion rates of undrained mires in Finland—application to boreal and subarctiv regions *Holocene* **12** 69–80

Vitt D H, Halsey L A and Zoltai S C 2000 The changing landscape of Canada's western boreal forest: the current dynamics of permafrost *Can. J. For. Res./Rev. Can. Rech. For.* **30** 283–7

Walter B P, Heimann M and Matthews E 2001 Modeling modern methane emissions from natural wetlands: 2. Interannual variations 1982–1993 *J. Geophys. Res.* **106** 34207–19

Wang J S, Logan J A, McElroy M B, Duncan B N, Megretskaia I A and Yantosca R M 2004 A 3D model analysis of the slowdown and interannual variability in the methane growth rate from 1988–1997 *Glob. Biogeochem. Cycles* **18** GB3011

Warner B G and Asada T 2006 Biological diversity of peatlands in Canada *Aquatic Sci.—Res. Across Bound.* **68** 240–53

Watts J D, Kimball J S, Bartsch A and McDonald K C 2014 Surface water inundation in the boreal-Arctic: potential impacts on regional methane emissions *Environ. Res. Lett.* **9** 075001

Yu Z 2006 Modeling ecosystems processes and pet accumulation in boreal peatlands *Boreal Peatland Ecosystems, Ecological Studies Analysis and Synthesis* vol 188 ed R K Wieder and H D Vitt (Berlin: Springer)

Zhang Y, Li C, Trettin C C, Li H and Sun G 2002 An integrated model of soil hydrology, and vegetation for carbon dynamics in wetland ecosystems *Glob. Biogeochem. Cycles* **16** 1061

Zhu X, Zhuang Q, Lu X and Song L 2014 Spatial scale-dependent land–atmospheric methane exchanges in the northern high latitudes from 1993–2004 *Biogeosciences* **11** 1693–704

Zhuang Q *et al* 2003 Carbon cycling in extratropical terrestrial ecosystems of the Northern Hemisphere during the 20th Century: a modeling analysis of the influences of soil thermal dynamics *Tellus* **55B** 751–76

Zhuang Q, McGuire A D, O'Neill K P, Harden J W, Romanovsky V E and Yarie J 2002 Modeling the soil thermal and carbon dynamics of a fire chronosequence in Interior Alaska *J. Geophys. Res.* **107** 8147

Zhuang Q, Melillo J M, McGuire A D, Kicklighter D W, Prinn R G, Steudler P A, Felzer B S and Hu S 2007 Net emissions of CH_4 and CO_2 in Alaska: implications for the region's greenhouse gas budget *Ecol. Appl.* **17** 203–12

Zhuang Q, Melillo J M, Kicklighter D W, Prinn R G, McGuire D A, Steudler P A, Felzer B S and Hu S 2004 Methane fluxes between terrestrial ecosystems and the atmosphere at northern high latitudes during the past century: a

retrospective analysis with a process-based biogeochemistry model *Glob. Biogeochem. Cycles* **18** GB3010

Zhuang Q, Melillo J M, Sarofim M C, Kicklighter D W, McGuire A D, Felzer B S, Sokolov A, Prinn R G, Steudler P A and Hu S 2006 CO_2 and CH_4 exchanges between land ecosystems and the atmosphere in northern high latitudes over the 21st century *Geophys. Res. Lett.* **33** L17403

Zhuang Q, Romanovsky V E and McGuire A D 2001 Incorporation of a permafrost model into a large-scale ecosystem model: evaluation of temporal and spatial scaling issues in simulating soil thermal dynamics *J. Geophys. Res.* **106** 33649–70